AIP Conference Proceedings, Volume 2033, Issue 1, 2018, Article number 030017
DOI:10.1063/1.5067033

The Design of Dust Barriers to Reduce Collector Mirror Soiling in CSP Plants

Christopher Sansom[1, a)], Peter King[1], Aránzazu Fernández-García[2], Heather Almond[1], Talib Kayani[1] and Houssame Boujjat[3]

[1]*Sustainable Manufacturing Systems Centre, Cranfield University, Bedford, Bedfordshire, MK43 0AL, UK*
[2]*CIEMAT-Plataforma Solar de Almería, Senes Road, Km. 4.5, P.O. Box 22, E04200 Tabernas, Almería, Spain*
[3]*CEA-INES, 73377 Le Bourget du Lac, France.*

[a)]Corresponding author: c.l.sansom@cranfield.ac.uk

Abstract. In this work we investigate, design, and evaluate a number of dust barrier designs that would be appropriate to reduce soiling of glass mirror solar collectors in the solar field of an existing CSP plant. The principal objective was to reduce the amount of soiling (and hence the amount of cleaning water consumed) by 50% in comparison with current cleaning procedures (considering particles of size >25μm). "Fluent" CFD software was used to model of a range of potential dust barrier shapes, sizes, and porosities. Airflows and wind loadings were analyzed in this way. A number of potential designs were then taken forward for experimental validation. Initial validation involved wind tunnel evaluation of a small number of potential designs, using a new wind tunnel specifically designed and built for this project. Larger-scale outdoor validation was carried out both at Cranfield University in the UK and at CIEMAT-PSA (Plataforma Solar de Almeria) in Spain. Initial results were independent of location and barrier shape and showed that the percentage of particles that were stopped completely or travelled less than 1m beyond the barrier was in the range 45.8 ± 5%.

INTRODUCTION

Dust barriers can control, shift and modify the wind flow. They can accelerate or decelerate the wind speed and produce degrees of turbulence. The impact of air flows on the dust particles themselves will depend on the size, shape, mass, charge, and chemical composition of the particles. Throughout this analysis it is assumed that smaller particles will follow the air flows. Our intention is to force those particles to either be brought to rest at or near the barrier or to be accelerated to a height whereby they cannot fall to ground within the solar field. Our intention is also to stop the larger particles at the barrier. However, there is little evidence for the deposition of larger particles (>250 μm) onto the solar collectors in CSP plants. Therefore they are not a major concern for removal during cleaning (note that this is not true when considering erosion, where the larger particles are the main cause of mirror damage). However the barriers designed on this project will also incorporate surfaces to decelerate larger particles, which can then fall under gravity to settle in the vicinity of the barrier. For a given location it is assumed that the barriers will be located in the direction from which the prevailing winds blow at the maximum speed according to the wind rose.

DUST BARRIER DESIGN AND CFD MODELLING

An example of the many CFD results obtained during the Ansys [1] modelling stage is shown in Fig. 1 below. A range of barrier shapes were analyzed, of porosities in the range 20-50%. As a concept, the approach was taken to create airflows that cause larger particles to fall to ground under gravity in the vicinity of the barrier whilst providing sufficient lift to accelerate smaller particles to a height where they are likely to pass over the solar field. As would be expected, the solid barrier accelerates the airflows over the barrier, but has the disadvantage of producing turbulent

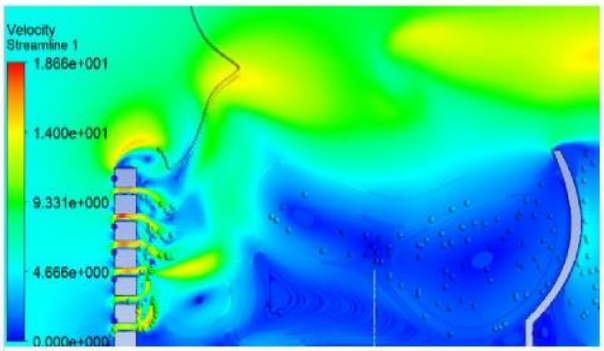

FIGURE 1a. CFD velocity contour for a porous barrier

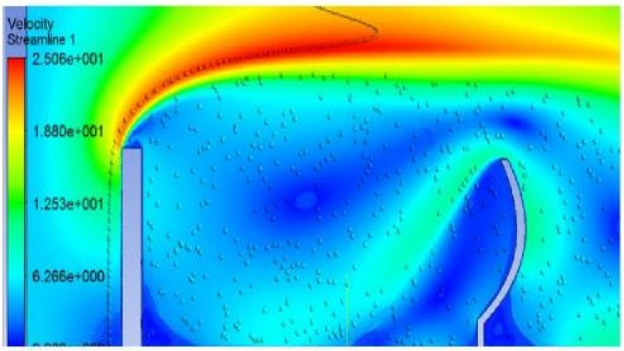

FIGURE 1b. CFD velocity contour for a solid barrier

flows beyond the barrier. These flows tend to pick up small ground-based particles which are then carried towards the collectors. In Fig 1a we see that the effect of a porous barrier is very different. The airflows beyond the barrier are more laminar in nature and there are no turbulent flows in the vicinity of the first row of collectors, as shown in the kinetic turbulent energy contours in Figure 2.

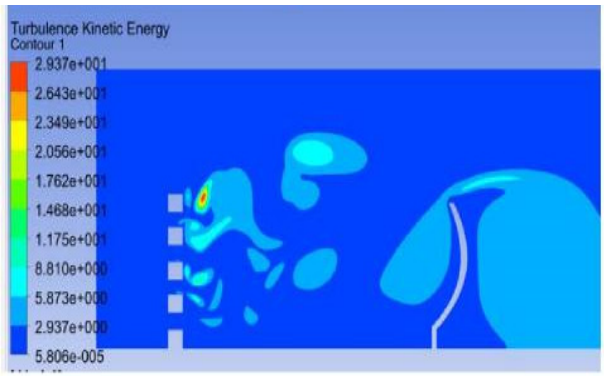

FIGURE 2a. Turbulent kinetic energy for a porous barrier

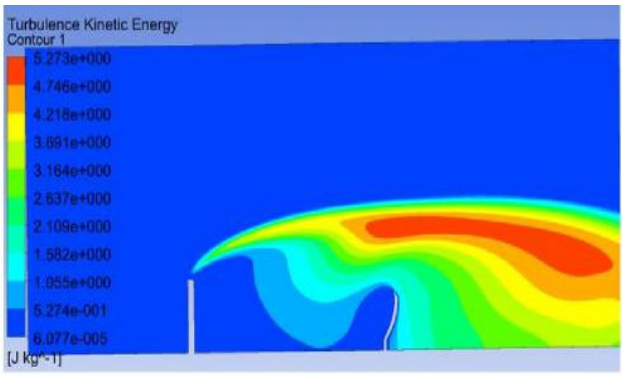

FIGURE 2b. Turbulent kinetic energy for a solid barrier

A solid barrier creates much more turbulence upstream which will promote the suspension of the particles in the air, whilst porosity restricts the larger eddies so as to minimise fluctuations in air flow. Porosity reduces the lateral components of mean velocity and of the larger turbulent eddies. Holes in the barriers will produce some turbulence of their own, with eddy sizes of the same order as the hole diameter. These eddies decay much faster than the large scale turbulence eddies. With porous barriers turbulence will be reduced, wind speed will decrease, the heaviest particles will settle out, and lighter particles will follow the streamlines. This is precisely the situation we are aiming to create. The effect of barrier porosity was also analyzed, as shown in Fig 3 below. In these simulations the porosity

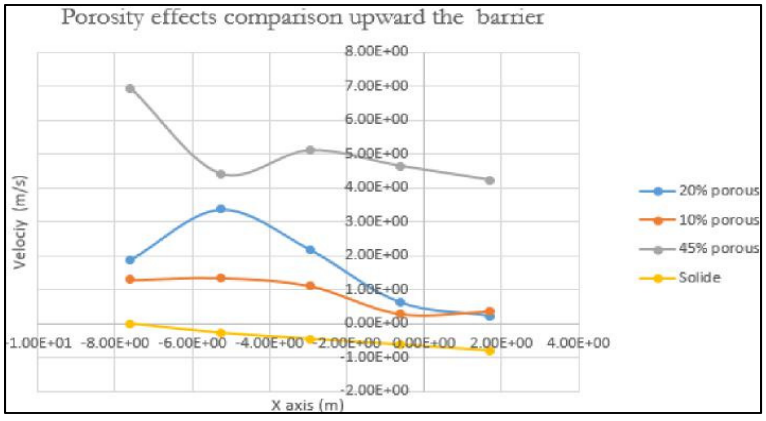

FIGURE 3. Airflow velocities for barrier porosities in the range 0-45%

of the barrier was allowed to vary from 0% (solid barrier) to 45%, these being the most promising values from previous work. Fig 3 shows that the velocity upstream decreases as the barrier becomes less porous. When the porosity is less than 10%, back flow and reverse zones are created due to the adverse pressure gradient, and turbulent kinetic energy increases which can promote the uptake of dust and sand from the ground. Ideally, porosity between 20% and 35% exhibits the best results in terms of decreasing the air velocity. These simulations provided the porosities for the models built for the wind tunnel experiments discussed in the next section. The best option to reduce the shear stress on the collector is to place the barrier as close as possible to the collector. However, then the sand and dust particles in the airflow will erode the collector mirror surfaces. Therefore placing the barrier at a distance from the first collector row of at least the barrier height is a sensible compromise.

Having fixed the range of porosity and the distance between the barrier and the collectors, we went on to study the influence of the barrier's shape upon stress. After much discussion and examination of existing barriers from the literature and from our own knowledge, plus brainstorming sessions, five barrier shapes were chosen to take forward. These are shown in Fig 4 below. The porosity (30%) and the barrier height (5.5m) were fixed during these simulations.

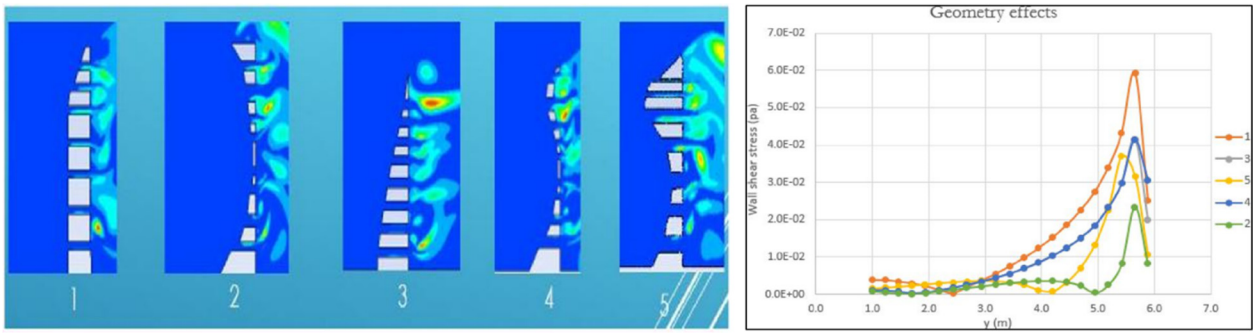

FIGURE 4. Five barrier shapes modelled

At a distance of 6m from the collectors, according to the simulations, shape number 2 best minimizes the wall shear stress by taking out the maximum energy from the wind, and reducing the upstream velocity. However, barrier designs 4 and 5 both exhibit a low stress distribution in comparison with other shapes, with the upper part of the barrier also acting to accelerate the air flow. Accelerating the airflow and providing lift at the upper part of the barrier is valuable for moving fine particles to a height where they could subsequently drift over the solar field. As all five shapes were of interest they were all retained in the next phase of the study, together with a plane barrier, making six in total.

DUST BARRIER TESTING

Wind Tunnel Testing

An initial validation of the CFD modelling involved wind-tunnel testing. To facilitate this a new 4m long open-loop and fan-driven wind tunnel was constructed at Cranfield University, with the concept shown in Fig 5a below [2-5].

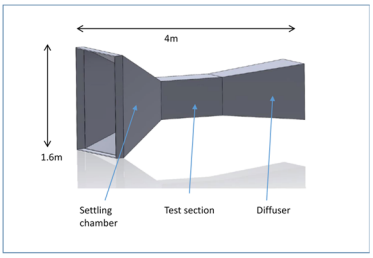

FIGURE 5a. Wind tunnel concept.

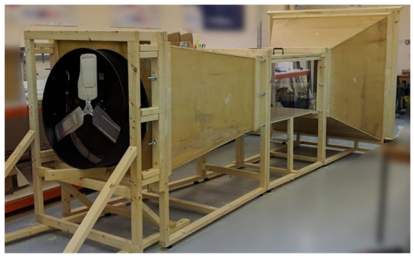

FIGURE 5b. Completed wind tunnel.

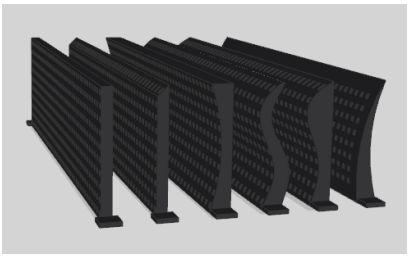

FIGURE 5c. Model barriers

The role of the settling chamber, which is upstream of the contraction section, is to eliminate swirl and unsteadiness from the airflow before it enters into the contraction section. The settling chamber has the largest cross-section of the wind tunnel and consists of an entrance section (ideally a bell-mouth shape although this is not essential), followed by a honeycomb or a series of screens. The purpose of the honeycomb is to remove any swirls in the incoming air flow and to minimise variations in both mean and fluctuating velocities. The primary design parameter for the honeycomb is the ratio of length to cell hydraulic diameter (L/D) and porosity (ratio of flow area to total area). The recommended L/D ratio for the honeycomb is between 6 and 8, that is, the cell length should be approximately 6 – 8 times its diameter. The honeycomb used was made from aluminium with holes of diameter 3.2 mm and total thickness of 20 mm giving an L/D ratio of 6.25. The Test Section of the tunnel is designed to have constant flow characteristics across its entire section (also known as the working-section). In order to install test models and measuring equipment, suitable access to the test section is an essential element of the design. In our case we have adopted a top-access design. The aim of the diffuser section is to convert the kinetic energy of the flow coming out of the test-section to pressure energy (before it leaves the diffuser) as efficiently as possible. The flow through the diffuser depends on its geometry, especially its area ratio (ratio of outlet area to the inlet area should be < 2.5), diffuser angle, wall contour and its cross-sectional shape. The area ratio of the diffuser and diffuser angle should be between 5° – 7° for controlling flow separation. Generally, the smaller the diffuser divergence angle, the more efficient the diffuser. At the exit, the cross-section is adapted to accommodate an axial fan. A Sealey HVD30 Industrial High Velocity Drum Fan was used to draw in air. (This is a 30in fan, running at 230V). Note that the fan is located at the diffuser end of the tunnel, with the honeycomb at the settling chamber end. Thus the fan draws in air from the far end of the tunnel, rather than blowing air down the tunnel from the diffuser end. This is a better configuration for linear and stable air currents. The wind tunnel was built by Roberts Enterprises for less than €2000, and is shown in Fig 5b. The model barriers are shown in Fig 5c, are 6cms in height ($1/100^{th}$ scale), and were fabricated in ABS plastic using a LulzBot Taz 3D printer. Wind speeds up to 7m/sec were measured in the test chamber using a Testo 425 thermal anemometer, and air streams were rendered visible using a smoke generator with an oil source. Figure 6 below shows the initial results from the wind tunnel trials. From both our CFD and wind tunnel results it is clear that it is not the shape of the barrier that is critically important in determining the airflow, but rather the porosity of the barrier, as described earlier. It also illustrates the limitations in considering

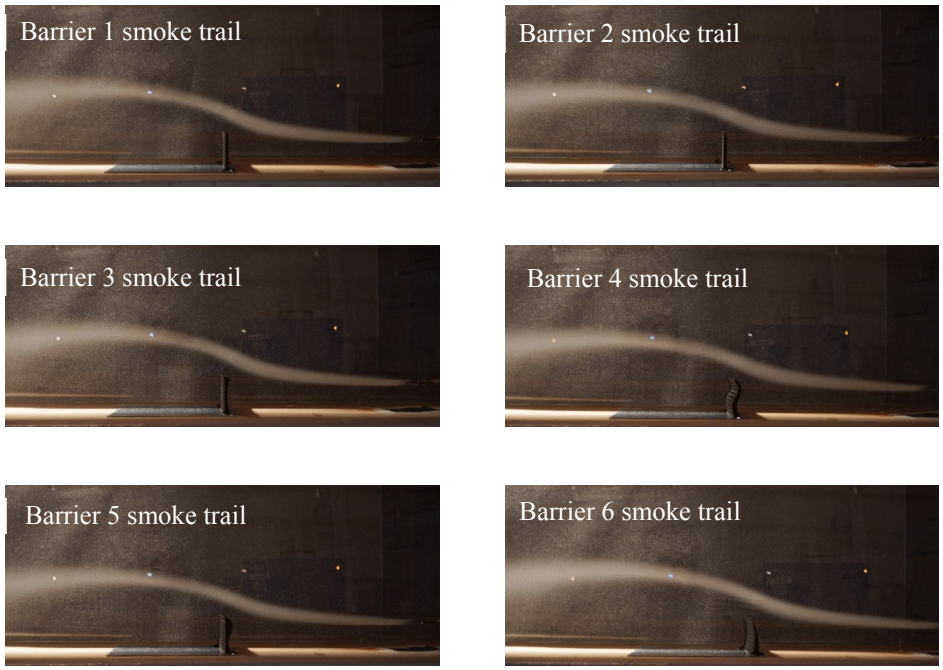

FIGURE 6. Wind tunnel results for all six barrier shapes

airflows when investigating the behavior of airborne particles, since the behavior of the former does not always predict the behavior of the latter. However, the wind tunnel results were useful in validating the CFD simulations of airflows over barriers and gave us the confidence to move forward to the next phase, namely the outdoor testing of small barriers in the presence of dust and sand.

Outdoor Testing

Before moving on to testing full-height barriers it was decided to test scaled-down versions in two outdoor locations, namely Cranfield University in the UK and CIEMAT-PSA in Spain. The experimental set-up is shown in Fig 7 below.

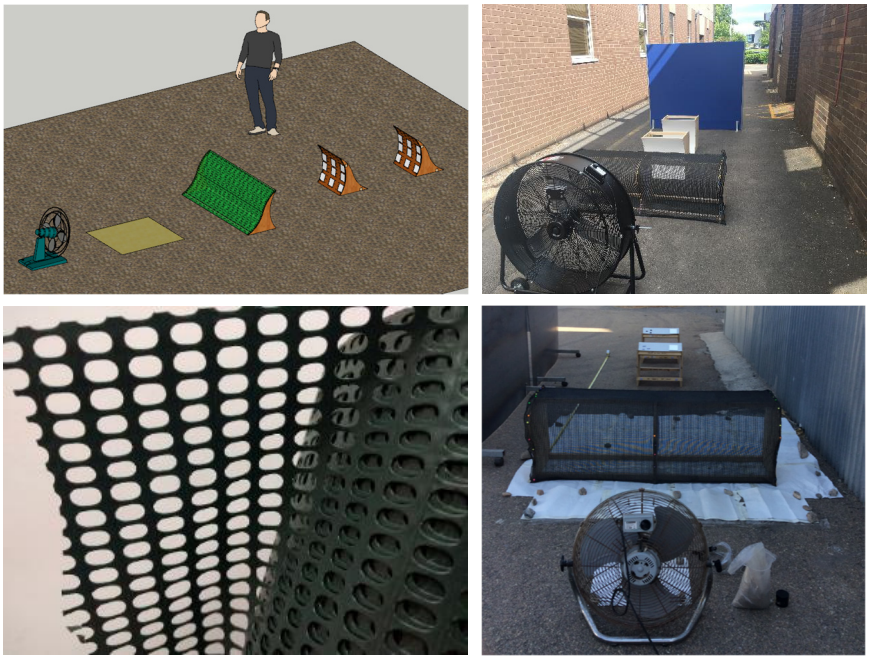

FIGURE 7. Outdoor testing of small dust barriers - with the following details: Schematic (upper left), Porous mesh (lower left), Cranfield experiment (upper right), PSA experiment (lower right)

As shown in the schematic drawing (Fig. 7, upper left), small barriers (0.5m high) were used. These consisted of wooden frames of the required shapes built by Roberts Enterprises covered with a porous and flexible sand-resistant plastic mesh (Fig. 7, lower left). The set-up at both Cranfield and the PSA was identical (Fig.7 upper right, Fig.7 lower right) , but there was considerable difference in ambient conditions and in the dust particles used. At the PSA, local ground-based dust was collected and sieved to ensure particle sizes <150 μm. At Cranfield the dust used was kiln-dried block-paving sand with particle sizes in the range 194-500 μm (all particle sizes as measured on the SEM at the PSA).

Our principal interest in this first phase of the outdoor experiments was to determine the effectiveness of a porous mesh barrier in preventing the dust from travelling more than a distance of (2 x barrier height) beyond the barrier (ie 1m in this case). The fan speed was set to produce airflows at the fan of 12 ms^{-1} as measured with a portable anemometer. The experiments were carried out at Cranfield in June 2017 and repeated at the PSA the following month. The quantities of dust were carefully measured at the start of the experiment using a fine balance. Particles were collected after the experiment in order to analyse their position relative to the barrier. Initial results were independent of location and barrier shape and indicated that the percentage of particles that failed to travel more than 1m beyond the barrier was in the range 45.8 ± 5%. This is a promising result, bearing in mind that our objective is to design a barrier to prevent more than 50% of airborne particles from reaching the collectors within a CSP plant. Experiments are now continuing to refine the barriers and to investigate the behavior of airborne particles that are not stopped at or nearby the barrier, together with their impact on the reflectance of glass mirrors.

CONCLUSIONS

Dust barriers for solar fields have been analysed, designed, built, and tested using CFD, wind tunnel validation, and outdoor testing experiments. We conclude that the dust barrier should be approximately the same height as the solar collectors, and should be placed at a distance from the first row of collectors that is approximately equal to its height. Porosities in the range 15-50% are suitable, with 30% giving the best results in terms or providing least turbulent air. A range of barrier shapes was considered. Initial experiments suggest that porosity is more important than barrier shape in reducing airflows in the vicinity of the barrier and in decelerating airborne particles. The results were independent of location and barrier shape and indicated that the percentage of particles that failed to travel more than 1m beyond the barrier was in the range 45.8 ± 5%. Future work will involve refinement of the barrier shape and porosity, reflectance measurements of glass samples to be placed behind the barrier, and the design of a larger barrier which will be compared with a natural barrier, such as a tree.

ACKNOWLEDGMENTS

The authors acknowledge EU funding from the Horizon 2020 project grant number 654479 “WASCOP” – Water Saving for Concentrating Solar Power”.

REFERENCES

1. ANSYS Fluent software; http://www.ansys.com/Products/Fluids/ANSYS-Fluent accessed on 27.03.17
2. Gharbanian K, Soltani MR, Manshadi D. Experimental investigation on turbulence reduction in subsonic wind tunnels. Aerospace Science and Technology. 2011 Mar; 15(2):137–47.
3. Mehta RD, Bradshaw P. Design rules for small low speed wind tunnels. The Aeronautical Journal. 1979 Nov; 83(827):443–9.
4. Arifuzzaman, MM. Design construction and performance test of a low cost subsonic wind tunnel. IOSR Journal of Engineering. 2012 Oct; 2(10):83–92.
5. Barlow JB, Rae WH, Pope A. Low-speed wind tunnel testing. 3rd Ed. Wind Tunnel Design. United States of America: John Wiley and Sons. 1999.